

# Learning Deficits in Aged Rats Related to Decrease in Extracellular Volume and Loss of Diffusion Anisotropy in Hippocampus

E. Syková,<sup>1,2</sup> T. Mazel,<sup>1,2</sup> R.U. Hasenöhr,<sup>3</sup>  
A.R. Harvey,<sup>4</sup> Z. Šimonová,<sup>1,2</sup> W.H.A.M. Mulders,<sup>5</sup>  
and J.P. Huston<sup>6,\*</sup>

<sup>1</sup>Department of Neuroscience, Second Medical Faculty,  
Charles University, Prague, Czech Republic

<sup>2</sup>Department of Neuroscience, Institute of Experimental  
Medicine AS CR, Prague, Czech Republic

<sup>3</sup>Department of Psychology, University of Hertfordshire,  
Hatfield, Hertfordshire, England, UK

<sup>4</sup>Department of Anatomy and Human Biology, University  
of Western Australia, Nedlands, Perth, Australia

<sup>5</sup>Department of Physiology, University of Western  
Australia, Nedlands, Perth, Australia

<sup>6</sup>Institute of Physiological Psychology and Center for  
Biological and Medical Research, University of Düsseldorf,  
Düsseldorf, Germany

**ABSTRACT:** The extracellular space (ECS) is the microenvironment of the nerve cells and an important communication channel, allowing for long-distance extrasynaptic communication between cells. Changes in ECS size, geometry, and composition have been reported in diverse (patho)physiological states, including aging. In the present study, real-time tetramethylammonium (TMA<sup>+</sup>) iontophoresis was used to quantify ECS diffusion parameters in different brain regions of adult and behaviorally characterized aged rats. Prior to ECS diffusion measurement, *superior* and *inferior* learners were selected from a large group of aged rats, according to their performance in the open-field water maze. The main finding was that the degree of impaired maze performance of old rats correlates, firstly, with decrease in ECS volume, loss of diffusion anisotropy in hippocampus, and degree of astrogliosis, and secondly, with disorganization of the astrocytic processes and reduction of hippocampal ECS matrix molecules. Importantly, no significant differences were found in the density of neurons in any region of the hippocampus or dentate gyrus. The alterations in hippocampal diffusion parameters evident in aged animals with severe learning deficits could account for the learning impairment, due to their effects on extrasynaptic volume transmission and/or on the “cross-talk” between synapses, which has been suggested to be involved in neural processes associated with learning and memory formation. *Hippocampus* 2002;12:469–479. © 2002 Wiley-Liss, Inc.

**KEY WORDS:** aging; extrasynaptic transmission; glycoproteins; tortuosity; volume fraction

## INTRODUCTION

Aging, Alzheimer's disease, and many other neurodegenerative diseases are accompanied by serious cognitive deficits, particularly impaired learning and memory loss. Cognitive decline in old age has been linked to changes in brain anatomy, morphology, volume, and functional deficits (reviewed in Grady and Craik, 2000). Nervous tissue, particularly in the hippocampus and cortex, is subject to various degenerative processes, including decrease in number and efficacy of synapses, neuronal loss, astrogliosis, and changes in extracellular matrix proteins. These and other changes not only affect the efficacy of signal transmission at synapses, but could also affect extrasynaptic volume transmission, mediated by the diffusion of transmitters as well as other substances through the volume of the extracellular space (ECS) (details in Agnati et al., 1995; Nicholson and Syková, 1998; Zoli et al., 1999).

For a long time, it was thought that the ECS comprises only a negligible part (5%) of the brain tissue and that it is formed by narrow, several nanometer-wide spaces as seen on electron microscopy images. Convincing evi-

Grant sponsor: Ministry of Education, Youth and Sports of the Czech Republic; Grant numbers: J13/98:111300004, LN00A65; Grant sponsor: Grant Agency of the Czech Republic; GACR 309/97/K048, GACR 309/99/0657; Grant sponsor: Deutsche Forschungsgemeinschaft; Grant number: Hu 306/11-3; Grant sponsor: NHMRC, Australia; Grant sponsor: Stanley Foundation, USA.

\*Correspondence to: J.P. Huston, Institute of Physiological Psychology, University of Düsseldorf, Universitätsstr. 1, D-40225 Düsseldorf, Germany. E-mail: huston@uni-duesseldorf.de

Accepted for publication 14 February 2001

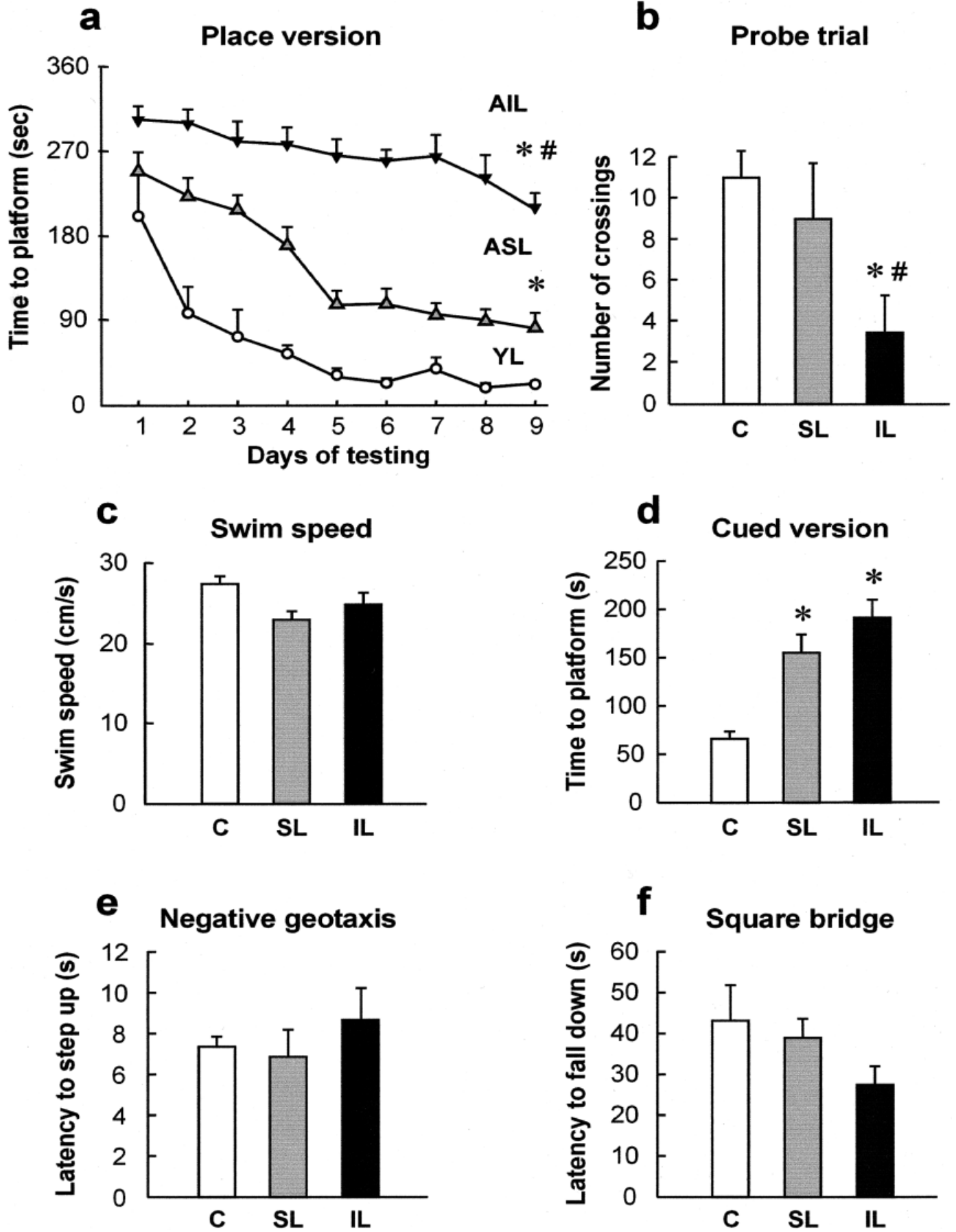


FIGURE 1

dence that in vivo the ECS is about 20% of the total tissue volume has accrued only recently (Syková, 1997; Nicholson and Syková, 1998) as a result of using a real-time iontophoretic method for diffusion analysis (Nicholson and Phillips, 1981). Besides the ECS volume, diffusion in the ECS is also dependent on 1) the apparent diffusion coefficient of a substance (ADC), which in nervous tissue is about 2.5 times lower than its diffusion coefficient in free solution ( $D$ ), and 2) nonspecific uptake ( $k'$ ), which describes the clearance of the substance from the ECS. The ratio between  $D$  and ADC gives a description of the ECS diffusion barriers, a factor called tortuosity  $\lambda = (D/ADC)^{0.5}$ , which has been shown to be related to the structure of the ECS in terms of macromolecular content, proteins, membranes, and fine cell (glia) processes (Syková et al., 1998).

We recently reported a decrease in ECS volume in the cortex, corpus callosum, and hippocampus of aged rats, accompanied by astrogliosis and a decrease in some extracellular matrix molecules (Syková et al., 1998). The question thus arises whether learning deficits during aging also involve the impairment of extrasynaptic volume transmission, mediated by the diffusion of neuroactive substances in the ECS. The present study was performed in the cortex, corpus callosum, and hippocampus of adult and behaviorally characterized aged rats, which were tested for memory loss. Here we show how the degree of a learning deficit that is associated with aging correlates with changes in ECS volume, geometry, and nonspecific uptake, three factors that describe the movement of substances diffusing from their source to their target. In the hippocampus and corpus callosum, diffusion is facilitated in one direction rather than in another, a phenomenon called diffusion anisotropy, which leads to a certain degree of specificity in extrasynaptic communication (Mazel et al., 1998; Wiesmann et al., 1999). Thus, we also examined whether this diffusion specificity is deficient in aged rats that show impaired spatial learning and whether the level of proficiency in learning is related to the severity of changes in diffusion parameters.

## MATERIALS AND METHODS

### Behavioral Screening

The water maze was a 185-cm-diameter black circular tank filled to a depth of 35 cm with opaque water at 20°C (Morris, 1984).

**FIGURE 1.** Behavioral profile of adult ( $C$ ,  $n = 18$ ) and behaviorally characterized aged rats (aged superior,  $SL$ ,  $n = 16$ ; aged inferior,  $IL$ ,  $n = 15$ ) included in the ECS parameter analyses. **a:** Time to escape onto the hidden platform over 9 days of training (four trials/day) in the place version of the maze. **b:** Number of times the rats swam over the former platform site in the 90-s probe trial. **c:** Overall swim speed in the place version of the maze. **d:** Time to escape onto the visible platform during cue training (total of four trials). **e:** Motor performance as assessed with (e) the test of negative geotaxis and (f) the square bridge. Data given are means  $\pm$  SEM. \* $P < 0.05$ , significantly different from adult rats. # $P < 0.05$ , significantly different from aged superior learners (Mann-Whitney U-test with Bonferroni's correction of the significance level for multiple comparisons).

Adult (3-month-old;  $n = 18$ ) and aged (28–31-month-old;  $n = 107$ ) Wistar rats were habituated to the maze by placing each subject into the apparatus for 90 s with no opportunity to escape. Commencing on the following day, rats were trained in the hidden-platform version of the task on 9 consecutive days (four trials/day). For each animal, an escape platform was fixed in the center of one quadrant of the maze 1.5 cm below water level and kept in the same location throughout training. Rats were placed in the maze from one of four equally spaced points along the perimeter of the pool. Entry points were randomly varied, with the criterion that each animal was placed in the maze at each entry point once during every four trials. After reaching the platform, rats were allowed to stay on it for 30 s; the next trial began 1 min later. A 90-s cutoff was imposed on all trials; if an animal failed to escape during this period, it was placed on the platform for 30 s. For each trial, time to platform and swim speed was measured. On day 11 (probe trial), the hidden platform was removed and the number of platform crossings, i.e., the number of times the rats swam through the area where the platform had been situated during place learning, was registered over a 90-s period. In the visible-platform version of the maze (day 12), animals were tested as described for the hidden-platform task, with the exception that a visible platform was placed 1.5 cm above the surface of the water in the center of the quadrant opposite to its original location (four trials). After the maze trials, motor performance was evaluated with a step-up test for negative geotaxis and with a square bridge. In the step-up test, the rat was placed on a 45° tilted platform (50 × 50 cm) with its nose facing the base; the time until it turned around by at least 135° was recorded. On the square bridge, the rat was placed in the middle of a wooden bridge (90 × 3.5 cm; 60 cm high); the time until it lost its balance and fell off the bridge was measured, with a 90-s cutoff imposed on the trials. After termination of the behavioral tests, 16 superior learners (SL) and 15 inferior learners (IL) were selected from the group of 107 aged animals for ECS diffusion parameter analysis. Criteria to select the two extreme groups were 1) performance across the 9 days in the hidden-platform version of the water maze and 2) performance during the probe trial (for methodological details, see Hasenöhrl et al., 1997).

### Diffusion Measurements

Fifteen to 45 days after the behavioral tests, the animals were anesthetized with sodium pentobarbital (65 mg/kg; i.p.), and additional small doses were used to maintain anesthesia during the experiment (Syková et al., 1998). The skull was opened 3–4 mm caudal from the bregma and 2–3 mm lateral from the midline, and the dura was removed. The animal was secured in a stereotaxic apparatus on a heated platform to maintain body temperature at 37–38°C. Artificial cerebrospinal fluid heated to 37°C was continually dripped onto the surface of the exposed skull to make a small pool over the brain surface. The ECS diffusion parameters, volume fraction  $\alpha$  ( $\alpha = \text{ECS volume}/\text{total tissue volume}$ ), tortuosity  $\lambda$ , and nonspecific uptake  $k'$ , were measured in the cortex, corpus callosum, and hippocampus along three orthogonal axes ( $x$ , mediolateral;  $y$ , rostrocaudal; and  $z$ , dorsoventral), using the real-time tetramethylammonium (TMA<sup>+</sup>) iontophoretic method (Nichol-

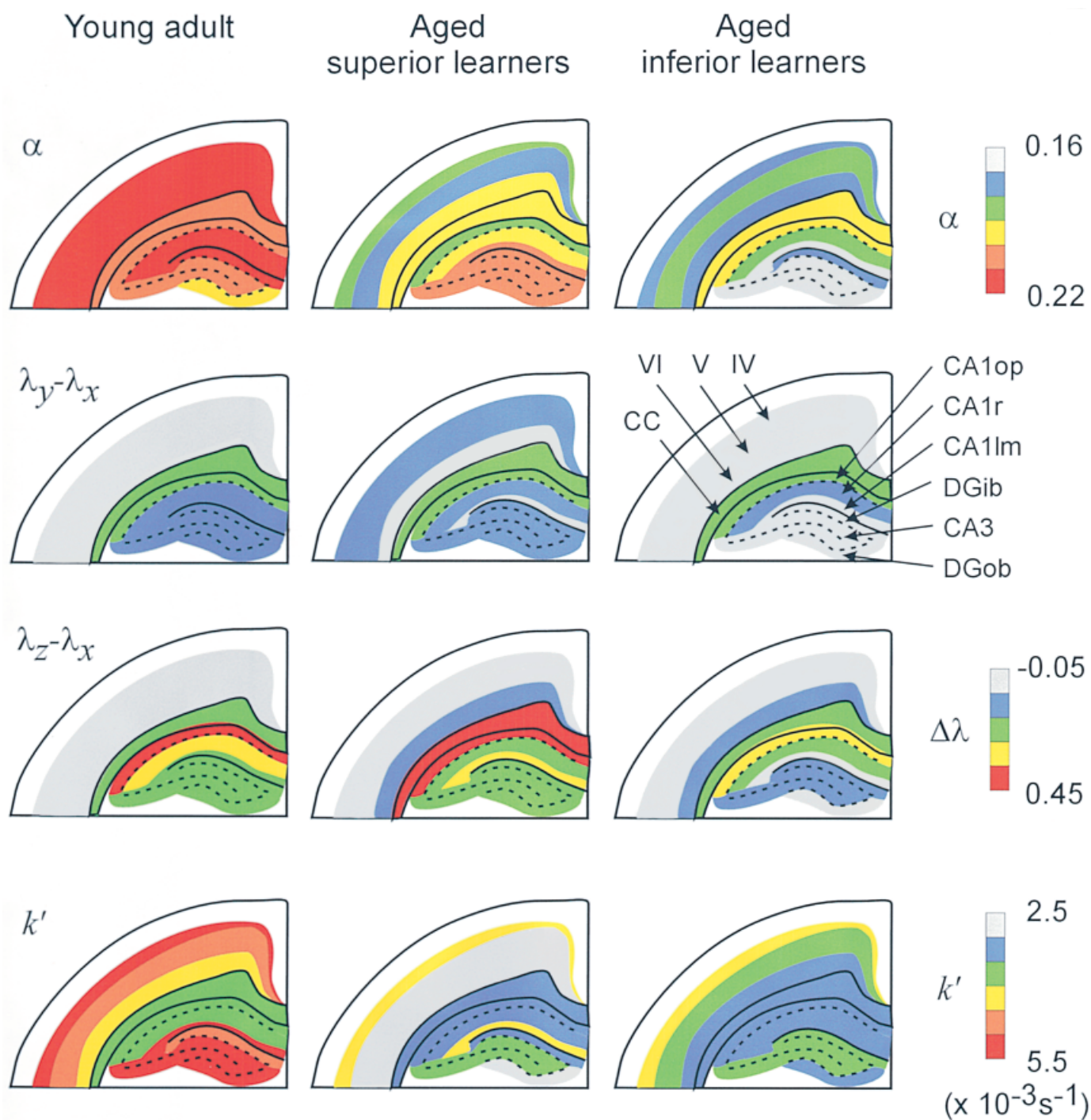


**FIGURE 2.** Pseudocolor images, showing the ECS diffusion parameters in individual structures of the brains of adult animals and aged superior and inferior learners. The following areas were selected: cortical layers IV, V, and VI, corpus callosum, CA1-stratum oriens including the alveus (CA1op), CA1-stratum radiatum (CA1r), CA1-stratum lacunosum moleculare (CA1lm), dentate gyrus-inner blade (DGib), CA3, and dentate gyrus-outer blade (DGob). The ECS vol-

ume fraction ( $\alpha$ ) and nonspecific TMA<sup>+</sup> uptake ( $k'$ ) in aged rats were lower than in adult animals in most areas studied. In the dentate gyrus of aged inferior learners, ECS volume was significantly lower than in superior learners. Anisotropy (difference between  $\lambda_x$ ,  $\lambda_y$ , and  $\lambda_z$ ) was much reduced or even eliminated in some areas of the hippocampus of aged inferior learners.

son and Phillips, 1981; Nicholson and Syková, 1998). The method is based on the iontophoretic application of TMA<sup>+</sup>, a small cation to which cell membranes are relatively impermeable,

and continuous measurement of its concentration 100–200  $\mu\text{m}$  away from the point of application. The ECS diffusion parameters are then determined by fitting the measured TMA<sup>+</sup> concentration

vs. time curves to a radial diffusion equation. Measurements were done using special electrode arrays prepared by gluing together a TMA<sup>+</sup>-selective microelectrode and two iontophoresis micropipettes with a tip separation of 100–200 μm, in such a way that the tips of the micropipettes and the TMA<sup>+</sup>-selective microelectrode formed a right angle, allowing us to measure simultaneously in either x and y or x and z or y and z directions (Mazel et al., 1998). TMA<sup>+</sup> diffusion curves were first recorded in 0.3% dilute agar gel ( $\alpha = 1 = \lambda$ ) to determine the transport number (n) and the free TMA<sup>+</sup> diffusion coefficient (D). Then the array was lowered 500 μm beneath the brain surface, where the first diffusion curves were recorded. Further recordings were made in 200-μm steps until a depth of 3,500 μm was reached. Diffusion curves in the cortex, corpus callosum, and hippocampus were analyzed to yield the apparent values of volume fraction ( $\alpha_x, \alpha_y, \alpha_z$ ), tortuosity  $\lambda_x, \lambda_y, \lambda_z$  in three perpendicular directions, and the nonspecific uptake term,  $k'$  (s<sup>-1</sup>). Only in the case of isotropic diffusion does  $\alpha = \alpha_x = \alpha_y = \alpha_z$ . In the case of anisotropic diffusion, however, the values are different, and the one true value of  $\alpha$  is calculated using the expression:  $\alpha = \alpha_x (\lambda_y \lambda_z / \lambda_x^2) = \alpha_y (\lambda_x \lambda_z / \lambda_y^2) = \alpha_z (\lambda_x \lambda_y / \lambda_z^2)$  (Rice et al., 1993; Prokopová et al., 1997; Mazel et al., 1998).

## Neuron Counting

After perfusion with 4% paraformaldehyde in 0.1 M phosphate buffer, the left hemispheres of 3 aged superior learners and 4 aged inferior learners were embedded in plastic (glycol methacrylate, Jung Historesin Plus, Leica). Consecutive series of sections, 1:15 or 1:5 series of 20 or 60 μm thickness, were cut in the horizontal plane, stained with Giemsa stain (Iniguez et al., 1995), dehydrated, and differentiated in 100% ethanol. The CA1 and CA3 regions of the hippocampus and dentate gyrus were defined and delineated as described in West et al. (1991). Neuron counts in these areas were obtained by using an optical fractionator (West et al., 1991). This method is not influenced by the size, shape, or orientation of the objects to be counted or shrinkage of the tissue. Volume measurements of the CA1, CA3, hilus, and granule-cell layer were performed by means of the Cavalieri principle (Gundersen and Jensen, 1987). All data were first analyzed using an F-test to compare variances of the means, and then analyzed using two-tailed Students' *t*-test.

## Immunohistochemistry

Immunohistochemical studies were undertaken on 9 adults, 9 aged SL, and 9 aged IL. Their brains were fixed with 4% paraformaldehyde; frozen sections (40 μm) were cut and immunostained (Syková et al., 1998). Astrocytes were identified using monoclonal antibodies to GFAP (Boehringer-Mannheim, Germany). Immunostaining for chondroitin sulfate proteoglycans (CSPG) was carried out using CS-56 antibodies (Sigma). For fibronectin staining, we used an antibody directed against the cell-attachment fibronectin fragment (Boehringer-Mannheim). After overnight incubation in the primary antibodies at 4°C, the floating sections were washed and processed using biotinylated anti-mouse secondary antibodies and the peroxidase-labelled avidin-biotin complex method (Vectastain Elite, Vector Laboratories, Burlingame, USA). Immune complexes were visualized using 0.05% 3,3'-diaminobenzidine

tetrachloride (Sigma). For the quantitative analysis of the density and distribution of immunostaining, the specimens were studied by optical densitometry, using a Zeiss KS 400 image analysis system. Regions of interest (ROI) in the CA3 pyramidal layers (CSPG) or in the granular-cell layer of dentate gyrus (fibronectin) were selected on the monitor, and the optical density (OD<sub>ROI</sub>) was determined. The subiculum (for CSPG) and the CA1 pyramidal cellular layer (for fibronectin) were used as reference values (OD<sub>REF</sub>). Densities of CSPG or fibronectin immunolabeling relative to OD<sub>REF</sub> were calculated as follows:  $(OD_{REF}/OD_{ROI} - 1) \times 100$  (Scheffler et al., 1997). Densitometric values of the three groups were compared using a two-tailed Students' *t*-test, and values were expressed as mean  $\pm$  SEM.

## RESULTS

### Behavioral Performance

Prior to ECS diffusion measurement, superior and inferior learners were selected from a large group of aged rats, according to their performance in different versions of the open-field water maze. The aged superior learners (aged SL) showed longer escape latencies and, thus, implicitly impaired performance in the place version of the task, but did not differ from adults on the platform crossing measure registered during the spatial probe (extinction) trial (Fig. 1a,b). The aged inferior learners (aged IL) were impaired on both measures in comparison with adult animals as well as with aged SL. The two subgroups of aged rats did not differ in swim speed in the course of place learning, in time to escape onto a visible platform in the cued version of the maze, or in motor performance, as assessed with a step-up test for negative geotaxis and a square bridge task (Fig. 1c–f). Thus, the differential degree of maze learning impairment evident in the subgroups of aged rats cannot readily be interpreted in terms of sensory and/or motor deficits, and is likely to be related to impairments of spatial learning and memory functions.

### Diffusion Parameters

The three ECS diffusion parameters, volume fraction  $\alpha$ , tortuosity  $\lambda$ , and nonspecific uptake  $k'$ , were measured along three orthogonal axes (x, transversal; y, sagittal; and z, dorsoventral) in the cortex, corpus callosum, and hippocampus. The pseudocolor images in Figure 2 present the differences in volume fraction  $\alpha$  in the identified anatomical regions of the adult animals and the aged SL and aged IL. It is apparent that in aged SL,  $\alpha$  was lower than in adult rats in all cortical layers, in the corpus callosum, and in CA1, but not in CA3 and the dentate gyrus. However, in aged IL,  $\alpha$  was even lower than in aged SL in cortical layers IV and VI and all hippocampal regions, including the dentate gyrus. Table 1 depicts the average values of ECS diffusion parameters obtained in the cortex, corpus callosum, and hippocampus of the adult and behaviorally characterized aged rats. In all these brain regions, adult rats show a typical volume fraction  $\alpha$  of about 0.21–0.22 (Mazel et al., 1998). The  $\alpha$  in

TABLE 1.

ECS Volume Fraction,  $\alpha$ , Tortuosity,  $\lambda$ , and Nonspecific Uptake,  $k'$  ( $10^{-3} \text{ s}^{-1}$ ), in the Cortex, Corpus Callosum, and Hippocampus of Adult Animals and Aged Superior and Inferior Learners\*

	Adult	Aged superior learners	Aged inferior learners
Cortex	$\alpha = 0.22 \pm 0.01$ (n = 176)	$\alpha = 0.18 \pm 0.01$ (n = 34) <sup>a</sup>	$\alpha = 0.18 \pm 0.01$ (n = 29) <sup>a</sup>
	$\lambda_{x,y,z} = 1.60 \pm 0.01$ (n = 176)	$\lambda_{x,y,z} = 1.59 \pm 0.02$ (n = 34)	$\lambda_{x,y,z} = 1.55 \pm 0.01$ (n = 29) <sup>ab</sup>
	$k' = 4.9 \pm 0.2$ (n = 176)	$k' = 2.9 \pm 0.2$ (n = 34) <sup>a</sup>	$k' = 3.5 \pm 0.2$ (n = 29) <sup>a</sup>
Corpus callosum	$\alpha = 0.21 \pm 0.01$ (n = 70)	$\alpha = 0.19 \pm 0.01$ (n = 18)	$\alpha = 0.20 \pm 0.01$ (n = 23)
	$\lambda_x = 1.47 \pm 0.01$ (n = 35)	$\lambda_x = 1.46 \pm 0.03$ (n = 10)	$\lambda_x = 1.49 \pm 0.01$ (n = 13)
	$\lambda_{y,z} = 1.68 \pm 0.01$ (n = 63) <sup>c</sup>	$\lambda_{y,z} = 1.77 \pm 0.06$ (n = 8) <sup>c</sup>	$\lambda_{y,z} = 1.64 \pm 0.03$ (n = 10) <sup>bc</sup>
Hippocampus	$k' = 3.5 \pm 0.2$ (n = 70)	$k' = 3.1 \pm 0.3$ (n = 18)	$k' = 3.4 \pm 0.4$ (n = 23)
	$\alpha = 0.22 \pm 0.01$ (n = 309)	$\alpha = 0.20 \pm 0.01$ (n = 51) <sup>a</sup>	$\alpha = 0.18 \pm 0.01$ (n = 50) <sup>ab</sup>
	$\lambda_x = 1.51 \pm 0.01$ (n = 118)	$\lambda_x = 1.51 \pm 0.02$ (n = 26)	$\lambda_x = 1.54 \pm 0.01$ (n = 34)
	$\lambda_y = 1.60 \pm 0.01$ (n = 100) <sup>c</sup>	$\lambda_y = 1.58 \pm 0.04$ (n = 18)	$\lambda_y = 1.57 \pm 0.02$ (n = 14)
	$\lambda_z = 1.74 \pm 0.02$ (n = 108) <sup>c</sup>	$\lambda_z = 1.74 \pm 0.04$ (n = 14) <sup>c</sup>	$\lambda_z = 1.64 \pm 0.03$ (n = 18) <sup>ab</sup>
	$k' = 4.6 \pm 0.1$ (n = 309)	$k' = 3.4 \pm 0.2$ (n = 51) <sup>a</sup>	$k' = 3.6 \pm 0.2$ (n = 50) <sup>a</sup>

\*Data are expressed as mean  $\pm$  SEM. Statistical significance between groups for each brain site was evaluated by one-way ANOVA. Significance was accepted at  $P < 0.05$ .

<sup>a</sup>Significant difference compared to adult animals.

<sup>b</sup>Significant difference between aged superior and inferior learners.

<sup>c</sup>Significant difference between  $\lambda_y$  and  $\lambda_x$  or  $\lambda_z$  and  $\lambda_y$ .

the cortex of both aged SL and aged IL was significantly lower than in young adult animals. However, only in the hippocampus was  $\alpha$  significantly lower in aged IL than in aged SL.

In the adult brain, diffusion in the somatosensory cortex is isotropic, while in the corpus callosum (Voříšek and Syková, 1997a) and hippocampus it is anisotropic (Mazel et al., 1998). Consistent with this finding, no significant differences between  $\lambda_x$ ,  $\lambda_y$ , and  $\lambda_z$  were observed in the cortex of adult rats; two different values of tortuosity were found in the corpus callosum, i.e., along the axons ( $\lambda_x$ ) and across the axons ( $\lambda_y$  and  $\lambda_z$ ); and three different values of tortuosity ( $\lambda_x$ ,  $\lambda_y$  and  $\lambda_z$ ) were found in the hippocampus. Table 1 demonstrates that the mean values of ECS tortuosity  $\lambda_{x,y,z}$  in the cortex,  $\lambda_{y,z}$  in the corpus callosum, and  $\lambda_z$  in the hippocampus were significantly lower in aged IL than in aged SL. Nevertheless, in both groups of aged rats, significant differences between the two  $\lambda$  values (diffusion anisotropy) were retained in the corpus callosum, a finding consistent with no apparent loss of myelin sheaths (Voříšek and Syková, 1997a). Importantly, decreases in both  $\lambda_y$  and  $\lambda_z$  led to a complete loss of anisotropy in the hippocampus of aged-IL only. The pseudocolor images in Figure 2 show that there was a greater loss of anisotropy in aged IL as compared to aged SL in all hippocampal regions. This was even more apparent when diffusion curves in all three axes were recorded in individual animals. Typical examples of diffusion curves recorded in the dentate gyrus are depicted in Figure 3. Keeping in mind that the more different the values of tortuosity ( $\lambda_x$ ,  $\lambda_y$ , and  $\lambda_z$ ) are, the greater the diffusion anisotropy, it is evident that anisotropy decreases with age, particularly in aged IL. The curves in Figure 3 clearly show that the loss of anisotropy in aged SL occurs along the y-axis, while in aged IL the loss occurs along both the y- and z-axes. Figure 3 also shows that  $\alpha$  in the dentate gyrus decreases with age (the diffusion

curves are bigger), particularly in the aged IL. In anisotropic tissue, the values of  $\alpha_x$ ,  $\alpha_y$ , and  $\alpha_z$  calculated from a single diffusion curve are substantially different from the actual ECS volume fraction  $\alpha$ . It is therefore evident that not taking anisotropy into account and measuring  $\alpha$  in only one direction must lead to incorrect values (McBain et al., 1990).

**FIGURE 3.** Experimental setup and typical diffusion curves in the hippocampus. **a:** Schema of experimental arrangement; a TMA<sup>+</sup>-selective double-barreled microelectrode was glued to two iontophoresis microelectrodes to allow for simultaneous measurements in the x- and y-axes. **b:** Anisotropic diffusion in dentate gyrus of an adult rat; TMA<sup>+</sup> diffusion curves (concentration-time profiles) were measured along three orthogonal axes (x, mediolateral; y, rostrocaudal; z, dorsoventral). The slower rise in the z than in the y direction and in the y than in the x direction indicates a higher tortuosity and more restricted diffusion. The amplitude of curves shows that TMA<sup>+</sup> concentration is much higher along the x-axis than along the y-axis and even higher than along z-axis. This can be explained if we realize that TMA<sup>+</sup> concentration decreases with the “diffusion distance” from the iontophoretic micropipette, and that the real “diffusion distance” is not  $r$  but  $\lambda r$ . Note that the actual ECS volume fraction  $\alpha$  is about 0.2 and can be calculated only when measurements are done in the x-, y-, and z-axes (see Materials and Methods). **c:** Anisotropy still persists in an aged rat that showed superior learning; diffusion curves are higher than in **b**, showing that  $\alpha$  is smaller. **d:** Anisotropy is almost lost in an aged severely impaired rat. Nonspecific uptake,  $k'$  ( $\times 10^{-3} \text{ s}^{-1}$ ), transport number,  $n$ , and electrode spacing,  $r$  (in  $\mu\text{m}$ ), are in **b:**  $k'_x = 4.4$ ,  $k'_y = 7.9$ ,  $k'_z = 7.8$ ,  $n_x = 0.35$ ,  $n_y = 0.31$ ,  $n_z = 0.30$ ,  $r_x = 156$ ,  $r_y = 150$ ,  $r_z = 169$ ; in **c:**  $k'_x = 1.4$ ,  $k'_y = 2.8$ ,  $k'_z = 1.3$ ,  $n_x = 0.22$ ,  $n_y = 0.23$ ,  $n_z = 0.21$ ,  $r_x = 150$ ,  $r_y = 157$ ,  $r_z = 170$ ; and in **d:**  $k'_x = 4.4$ ,  $k'_y = 3.9$ ,  $k'_z = 2.1$ ,  $n_x = 0.20$ ,  $n_y = 0.21$ ,  $n_z = 0.25$ ,  $r_x = 145$ ,  $r_y = 159$ ,  $r_z = 160$ .

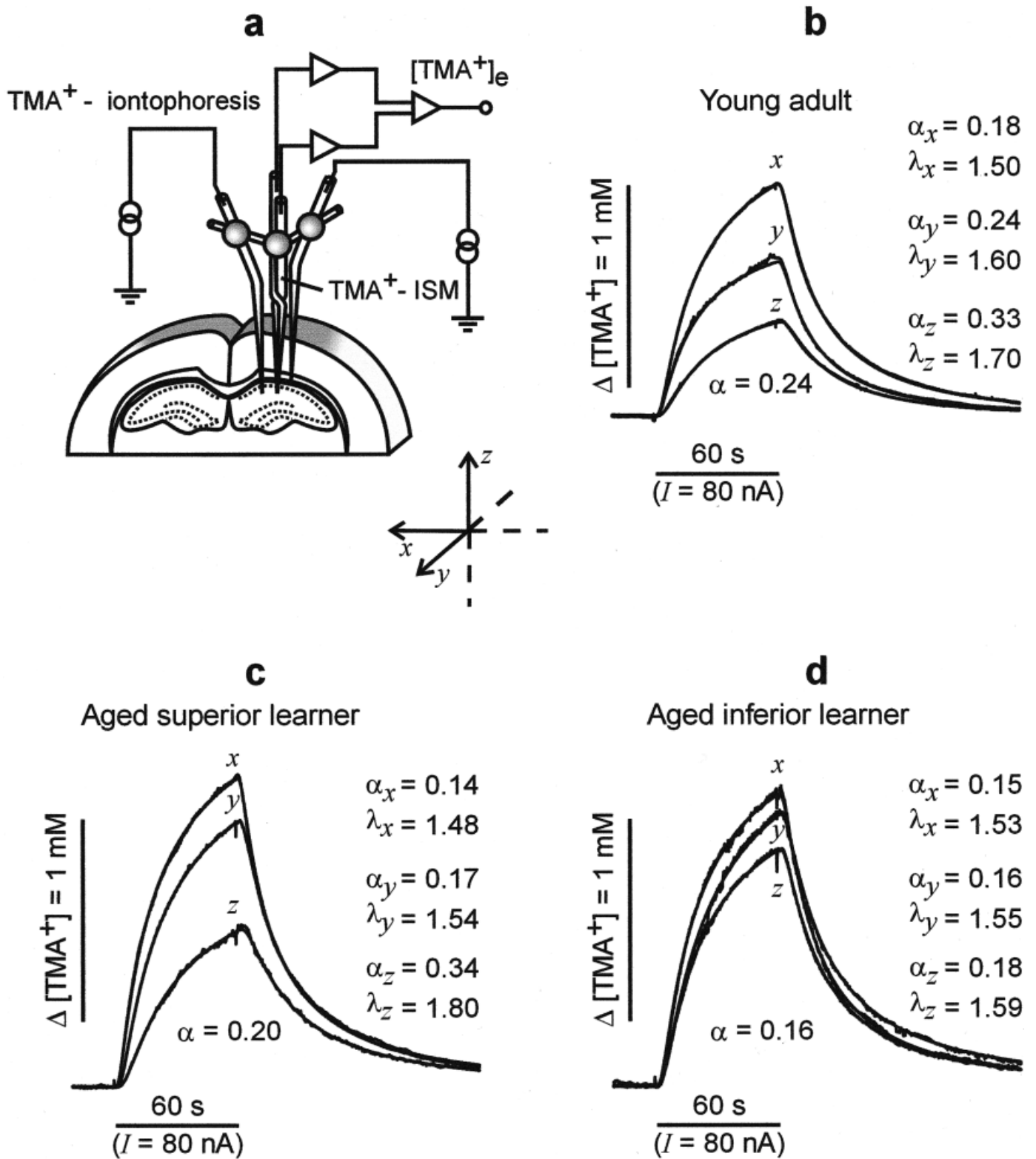


FIGURE 3

One of the other striking changes we found was a reduction of nonspecific TMA<sup>+</sup> uptake ( $k'$ ) in the cortex and hippocampus of aged rats, independent of the degree of learning impairment. Non-

specific uptake was reduced mainly in cell-body-rich areas and not in the corpus callosum, suggesting that cellular, presumably glial, uptake was reduced.

## Neuron Counts, Astrocytes, and Extracellular Matrix

In order to study possible morphological concomitants of the changes in ECS diffusion parameters, brains of aged IL and aged SL were subjected to detailed histological analysis. Congruent with the results of other studies (Rapp and Gallagher, 1996), quantification of the number of neurons in the CA1 and CA3 of the hippocampus and in the hilus revealed no significant differences between aged SL and aged IL. Counts in the granule-cell layer (GCL) of aged SL, however, revealed that this region on average contained more neurons ( $1.705 \pm 0.18$ , mean unilateral value in millions  $\pm$  SEM,  $n = 3$ ) than in aged IL ( $1.098 \pm 0.13$ ,  $n = 4$ ;  $P < 0.05$ ). Similar to the results of the neuron counts, statistical analysis revealed no differences between the two aged groups with respect to the average volume of CA1, CA3, or the hilus. The GCL in aged SL was significantly larger ( $1.34 \pm 0.15$ , mean unilateral value in  $\text{mm}^3 \pm$  SEM,  $n = 3$ ) than in aged IL ( $0.93 \pm 0.07$ ,  $n = 4$ ). Importantly, no significant differences between aged SL and aged IL were evident in the density of neurons in any region of the hippocampus or dentate gyrus (DG). In the granule-cell layer, for example, the mean neuronal densities were  $1.272 \times 10^6/\text{mm}^3$  and  $1.181 \times 10^6/\text{mm}^3$ , respectively.

Staining for the astrocytic marker GFAP revealed astrogliosis in the brains of both groups of aged rats (Nichols et al., 1993). These changes might explain the observed decrease in ECS volume fraction if there was an increase in the relative cell density of glia, particularly astrocytes. In the hippocampus, the typical radial organization of astrocytic processes observed in the CA1, CA3, and DG of adult rats was clearly disrupted in all aged SL, and was totally absent in aged IL (Fig. 4a–c). This loss of radial organization could in part explain the loss of diffusion anisotropy.

It was shown previously that the decrease in tortuosity that accounts for the loss of anisotropy could also be due to changes in the molecules of the extracellular matrix (Syková et al., 1998, 2000). Figure 4d–i shows immunostaining for chondroitin sulphate proteoglycans as well as for fibronectin in adults, aged SL, and aged IL. There was a clear decrease in the staining around neurons and their processes (forming the so-called perineuronal nets), with only a few perineuronal nets around neurons in the CA1, CA3, and DG of aged SL, but a complete loss of staining in aged rats with inferior performance. Figure 4j shows the significant differences between both adults and aged SL as well as between aged SL and aged IL as revealed by quantitative analysis of the density of CSPG immunolabeling, while Figure 4k shows a significant decrease in immunolabeling for fibronectin in aged-IL only.

## DISCUSSION

Our study used the *in vivo* TMA<sup>+</sup> method to evaluate diffusion parameters in the aging cortex, corpus callosum, and hippocampus. The ECS volume fraction and nonspecific TMA<sup>+</sup> uptake in the cortex and hippocampus of aged rats were significantly lower

than in young adults. Moreover, there was a significant difference between mildly and severely behaviorally impaired rats, which was particularly apparent in the hippocampus. The ECS in the dentate gyrus of severely impaired rats was significantly smaller than in mildly impaired rats. In addition, anisotropy in the hippocampus of severely impaired rats, particularly in the dentate gyrus, was much reduced, while a substantial degree of anisotropy was still present in aged rats with a better learning performance.

We confirm the already published significant decrease in ECS volume fraction in the cortex and hippocampus during aging (Syková et al., 1998). Thus, volume fraction decreases throughout life, with the first steep decrease occurring in early postnatal development (Lehmenkühler et al., 1993; Voříšek and Syková, 1997b), and the second during aging (Syková et al., 1998). The larger ECS (30–45%) in the first days of rat postnatal development can be attributed to incomplete neuronal migration, gliogenesis, angiogenesis, and the presence of large extracellular matrix proteoglycans, particularly hyaluronic acid, which due to the mutual repulsion of its highly negatively charged branches occupies a great deal of space and holds the cells apart from each other. The ensuing decrease in ECS size could be explained by the disappearance of a significant part of the ECS matrix, neuron migration, development of dendritic trees, rapid myelination, and proliferation of glia.

Some of these processes are also observed during aging. The most important of these besides neuronal degeneration probably include the further loss of extracellular matrix and astrogliosis. Indeed, we observed a decrease of chondroitin sulfate proteoglycan staining in the hippocampus of aged SL and almost a complete loss of staining in aged IL, while immunolabeling for fibronectin was reduced in the severely impaired aged rats only. This finding is of interest in light of a recent study showing that proteoglycan substitution by chronic icv infusion of biglycan, a small chondroitin sulfate proteoglycan, as well as its chondroitin-6-sulfate side chains, can significantly improve the maze performance of behaviorally impaired old rats (Huston et al., 2000). Astrogliosis in aged rats was revealed by enhanced staining for the astrocytic marker GFAP. These changes might explain the observed decrease in ECS volume fraction if there was an increase in the relative cell density of glia, particularly astrocytes. Furthermore, in the hippocampus, the typical radial organization of astrocytic processes was clearly disrupted in aged SL and totally absent in aged IL. This loss of radial organization could in part explain the loss of diffusion anisotropy.

Tortuosity characterizes the prolongation of the diffusion path of a certain molecule in tissue as compared to a free solution. It is influenced by many factors which we presently cannot separate, e.g., extracellular space size and geometry, macromolecules including the extracellular matrix, or molecules with fixed negative surface charges. In a purely geometrical way of thinking, one would expect that tortuosity should increase if the ECS size gets smaller. This was actually observed in most *in vitro* experiments following the application of hypotonic solutions or drugs that cause acute cellular swelling. However, in our present study, the average tortuosity (the mean of  $\lambda_x$ ,  $\lambda_y$ , and  $\lambda_z$ ) either was the same as in young adults or even slightly reduced. This suggests that other factors are involved, particularly the loss of extracellular matrix, shortened



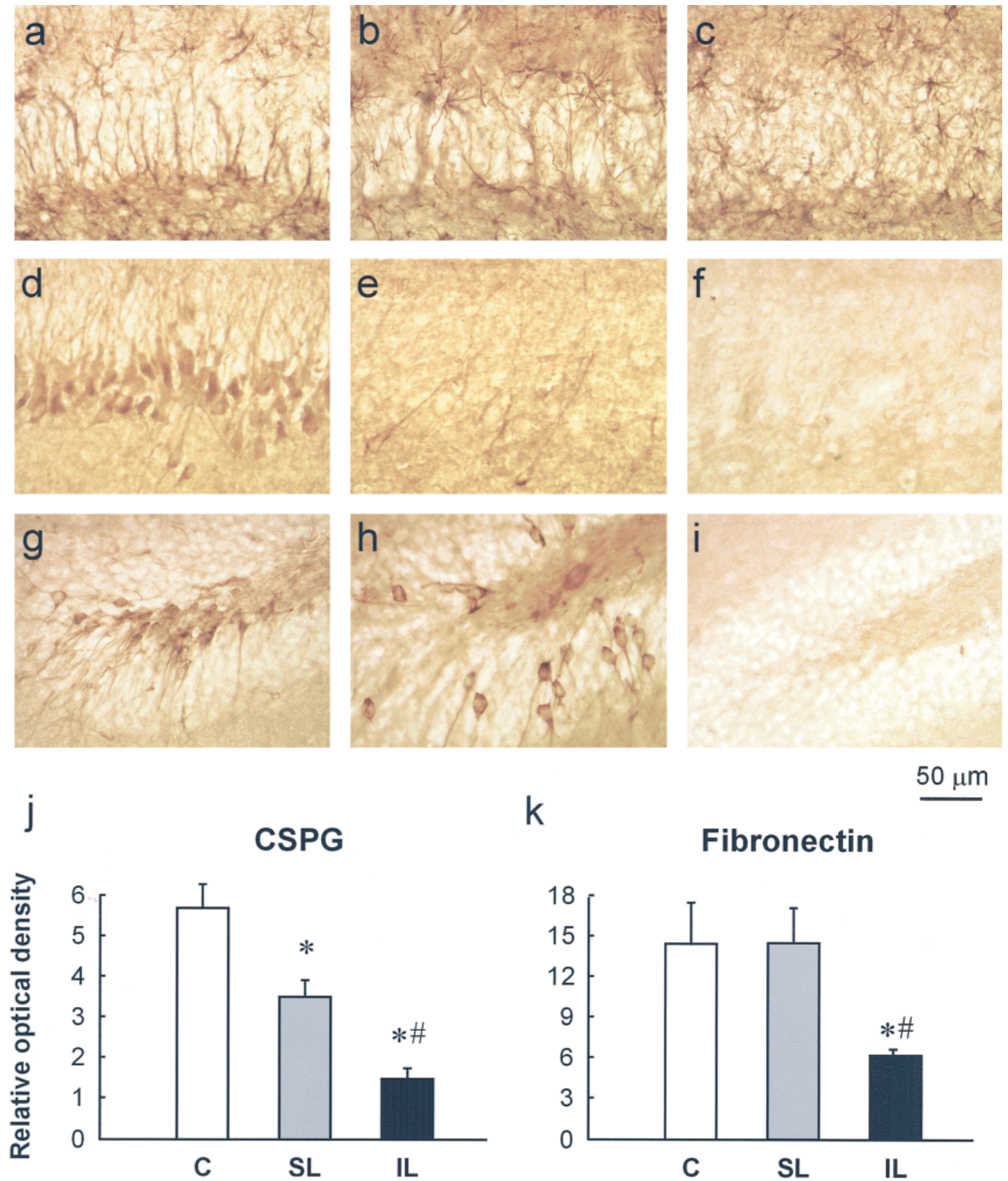


**FIGURE 4.** Structural changes in aged superior and inferior learners. a–c: Astrocytes in the dentate gyrus (inner blade) of a adult rat, an aged SL, and an aged IL. Note the loss of radial organization of the astrocytic processes in aged IL. Staining for chondroitin sulfate proteoglycans (CSPG) in the hippocampal CA3 region (d–f) and fibronectin in dentate gyrus (g–i) shows a decrease in perineuronal

staining in aged SL and a loss in aged IL. The graphs show the relative optical densities of CSPG (j) and fibronectin cell attachment fragment (k) immunoreactivity. Note the significant decrease in CSPG immunoreactivity between each group and the decrease in fibronectin immunoreactivity in aged-IL only.

astrocytic processes and their reduced branching, and the reduced branching of neuronal processes (Syková et al., 1998, 2000). Another way to explain our results is based on a histological study by Schmolke (1996), who divided the cortical nervous tissue into three compartments: dendrite bundles, axonal bundles, and the neuropil between them. In aged animals, he found a significant reduction of the neuropil, which is known to have larger extracellular spaces and higher tortuosity than the other two compartments.

Tortuosity is not a scalar, as is volume fraction or uptake. It is a tensor, generally having six different components characterizing how the flux of a substance along one axis is influenced by its concentration gradient along another axis. It can be reduced to its three diagonal components if a suitable system of coordinates is selected (our  $z$ -axis is perpendicular to the anatomical layers of the cortex, corpus callosum, and hippocampus). Isotropic diffusion is defined by a lack of significant differences between these three diagonal components. Isotropic diffusion was found in the cortex of both adult and aged rats. Anisotropic diffusion was found in the corpus callosum (with diffusion facilitated along the myelinated fibers) and hippocampus. The anisotropy in corpus callosum did not change during aging. However, there were significant differences in the degree of anisotropy found in the hippocampus of the three groups of animals. In adults, all three diagonal components were significantly different, whereas in aged animals the difference between  $\lambda_x$  and  $\lambda_y$  was eliminated. Moreover, in severely impaired aged rats, the difference between  $\lambda_z$  and  $\lambda_x$  or  $\lambda_y$  was markedly reduced, particularly in the dentate gyrus. This decrease in anisotropy might again be due to a loss of extracellular matrix and fine astrocytic processes that also lose their regular organization, particularly in severely impaired animals (Syková et al., 1998). It was shown recently that superfusion of rat cortical slices or isolated rat spinal cords with a solution containing either 40 kDa or 70 kDa dextran or hyaluronic acid results in a significant increase in  $\lambda$ , while a single intracortical injection of the enzymes neuraminidase or chondroitinase ABC results in a decrease in tortuosity (Syková et al., 2000). Anisotropy might be important for extrasynaptic transmission by channeling the flux of substances in a preferential direction. Its loss may severely disrupt extrasynaptic communication in the central nervous system, which has been suggested to play an important role in memory formation (Syková and Nicholson, 1997; Syková et al., 1998).

One of the most striking changes we observed was the reduction of nonspecific TMA<sup>+</sup> uptake ( $k'$ ) in the cortex and hippocampus of aged rats, independent of the degree of learning impairment. A similar decrease was also found in astroglial tissue (Syková et al., 1999; Roitbak and Syková, 1999). The underlying mechanism of TMA<sup>+</sup> uptake may include transfer into cells, loss across the blood-brain barrier (BBB), or binding to cellular surfaces or to negatively charged molecules of the extracellular matrix. During aging, transfer into cells might decrease due to reduced pinocytosis (stiffer membranes due to a higher proportion of cholesterol). Furthermore, the BBB might be less permeable, and binding to cellular surfaces due to reduced membrane potential might be decreased, as might binding to the extracellular matrix due to its loss.

It is also interesting that uptake was reduced mainly in cell-body-rich areas and not in the corpus callosum.

In conclusion, our results indicate that the degree of learning impairment in aged rats is related to dysfunctional changes in ECS diffusion parameters, particularly in the hippocampus, which may occur secondary to astrogliosis and to changes in the organization of cellular processes and in extracellular matrix molecules. Anisotropy in the hippocampus may help to facilitate the extracellular diffusion of neurotransmitters and neuromodulators to regions occupied by their high-affinity extrasynaptic receptors and have crucial importance for the specificity of extrasynaptic volume transmission. The importance of anisotropy for the spillover of glutamate or GABA, for cross-talk between synapses, and for LTP and LTD has also been proposed (Kullmann et al., 1996; Asztely et al., 1997). The observed loss of anisotropy in senescent rats could therefore lead to impaired hippocampal functioning. Furthermore, it has been suggested that a decrease in ECS size and non-specific uptake could be responsible for the greater susceptibility of the aged brain to pathological events (particularly ischemia), the more limited recovery of affected tissue after insult, the limited penetration of neuroactive substances through less permissive aged tissue, and the poorer outcome of clinical therapy (Syková et al., 1998). Here we suggest that the observed changes in ECS diffusion parameters can significantly influence extrasynaptic communication and therefore contribute to age-related learning deficits.

## REFERENCES

- Agnati LF, Zoli M, Stromberg I, Fuxe K. 1995. Intercellular communication in the brain: wiring versus volume transmission. *Neuroscience* 69:711–726.
- Asztely F, Erdemli G, Kullmann DM. 1997. Extrasynaptic glutamate spillover in the hippocampus: dependence on temperature and the role of active glutamate uptake. *Neuron* 18:281–293.
- Grady CL, Craik FI. 2000. Changes in memory processing with age. *Curr Opin Neurobiol* 10:224–231.
- Gundersen HJG, Jensen EB. 1987. The efficiency of systematic sampling in stereology and its prediction. *J Microsc* 147:229–263.
- Hasenöhrl RU, Söderström S, Mohammed AH, Ebendal T, Huston JP. 1997. Reciprocal changes in expression of mRNA for nerve growth factor and its receptors TrkA and LNGFR in brain of aged rats in relation to maze learning deficits. *Exp Brain Res* 114:205–213.
- Huston JP, Weth K, De Souza Silva A, Junghans U, Müller HW, Hasenöhrl RU. 2000. Facilitation of learning and long-term ventral pallidal-cortical cholinergic activation by proteoglycan biglycan and chondroitin sulfate C. *Neuroscience* 100:355–361.
- Iniguez C, Gayoso MJ, Carreres J. 1985. A versatile and simple method for staining nervous tissue using Giemsa dye. *J Neurosci Methods* 13:77–86.
- Kullmann DM, Erdemli G, Asztely F. 1996. LTP of AMPA and NMDA receptor-mediated signals: evidence for presynaptic expression and extrasynaptic glutamate spill-over. *Neuron* 17:461–474.
- Lehmenkühler A, Syková E, Svoboda J, Zilles K, Nicholson C. 1993. Extracellular space parameters in the rat neocortex and subcortical white matter during postnatal development determined by diffusion analysis. *Neuroscience* 55:339–351.
- Mazel T, Šimonová Z, Syková E. 1998. Diffusion heterogeneity and anisotropy in rat hippocampus. *Neuroreport* 9:1299–1304.

- McBain CJ, Traynelis SF, Dingledine R. 1990. Regional variation of extracellular space in the hippocampus. *Science* 249:674–677.
- Morris RGM. 1984. Developments of a water-maze procedure for studying spatial learning in the rat. *J Neurosci Methods* 11:47–60.
- Nichols NR, Day JR, Laping NJ, Johnson SA, Finch CE. 1993. GFAP mRNA increases with age in rat and human brain. *Neurobiol Aging* 14:421–429.
- Nicholson C, Phillips JM. 1981. Ion diffusion modified by tortuosity and volume fraction in the extracellular microenvironment of the rat cerebellum. *J Physiol (Lond)* 321:225–257.
- Nicholson C, Syková E. 1998. Extracellular space structure revealed by diffusion analysis. *Trends Neurosci* 21:207–215.
- Prokopová S, Vargová L, Syková E. 1997. Heterogeneous and anisotropic diffusion in the developing rat spinal cord. *Neuroreport* 8:3527–3532.
- Rapp PR, Gallagher M. 1996. Preserved neuron number in the hippocampus of aged rats with spatial learning deficits. *Proc Natl Acad Sci USA* 93:9926–9930.
- Rice ME, Okada YC, Nicholson C. 1993. Anisotropic and heterogeneous diffusion in the turtle cerebellum: implications for volume transmission. *J Neurophysiol* 70:2035–2044.
- Roitbak T, Syková E. 1999. Diffusion barriers evoked in the rat cortex by reactive astrogliosis. *Glia* 28:40–48.
- Scheffler B, Faissner A, Beck H, Behle K, Wolf HK, Wiestler OD, Blümcke I. 1997. Hippocampal loss of tenascin boundaries in Ammon's horn sclerosis. *Glia* 19:35–46.
- Schmolke C. 1996. Tissue compartments in laminae II–V of rabbit visual cortex—three-dimensional arrangement, size and developmental changes. *Anat Embryol (Berl)* 193:15–33.
- Syková E. 1997. The extracellular space in the CNS: its regulation, volume and geometry in normal and pathological neuronal function. *Neuroscientist* 3:28–41.
- Syková E, Mazel T, Šimonová Z. 1998. Diffusion constraints and neuron-glia interaction during aging. *Exp Gerontol* 33:837–851.
- Syková E, Vargová L, Prokopová S, Šimonová Z. 1999. Glial swelling and astrogliosis produce diffusion barriers in the rat spinal cord. *Glia* 25:56–70.
- Syková E, Mazel T, Vargová L, Voříšek I, Prokopová-Kubinová Š. 2000. Extracellular space diffusion and pathological states. *Prog Brain Res* 125:155–178.
- Voříšek I, Syková E. 1997a. Ischemia-induced changes in the extracellular space diffusion parameters, K<sup>+</sup> and pH in the developing rat cortex and corpus callosum. *J Cereb Blood Flow Metab* 17:191–203.
- Voříšek I, Syková E. 1997b. Evolution of anisotropic diffusion in the developing rat corpus callosum. *J Neurophysiol* 78:912–919.
- West MJ, Slomianka L, Gundersen HJG. 1991. Unbiased stereological estimation of the total number of neurons in the subdivisions of the rat hippocampus using the optical fractionator. *Anat Rec* 231:482–497.
- Wiesmann UC, Clark CA, Symms MR, Barker GJ, Birnie KD, Shorvon SD. 1999. Water diffusion in the human hippocampus in epilepsy. *Magn Reson Imaging* 17:29–36.
- Zoli M, Jansson A, Syková E, Agnati LF, Fuxe K. 1999. Intercellular communication in the central nervous system. The emergence of the volume transmission concept and its relevance for neuropsychopharmacology. *Trends Pharmacol Sci* 20:142–150.